Experimental study on shear performance and bearing capacity of prestressed concrete T-BEAMS

Estudio experimental sobre el rendimiento y la capacidad de carga de cizallamiento para vigas en T de hormigón pretensado

Feng Haoxiong[1*,2], Yi Weijian[2]

[1] College of Civil Engineering, Hunan City University, Yingbin East Road 518#, Hunan, 413000, Yiyang, China
[2] College of Civil Engineering, Hunan University, Lushan South Road, Hunan , 410082, Changsha, China.
* Corresponding author,email: fhx2437@163.com

DOI: http://dx.doi.org/10.6036/9655 | Recibido: 31/01/2020 • Inicio Evaluación: 31/01/2020 • Aceptado: 01/04/2020

RESUMEN

- Las vigas en T de hormigón pretensado tienen un complejo mecanismo de cizallamiento y su comportamiento en el cizallamiento está influenciado por varios factores, como el ancho del ala y el pretensado. El rendimiento de cizallamiento de las vigas en T de hormigón pretensado no se ha resuelto por completo. Este estudio diseñó y estableció nueve vigas en T de hormigón pretensado y una viga en T ordinaria de hormigón armado para investigar la influencia de la anchura del ala y el número y ángulo de flexión de los tendones pretensados en la capacidad de carga de cizallamiento de las vigas en T de hormigón. Se midió el desarrollo de la grieta, la forma de la falla, la deformación en la mitad del tramo y la tensión del hormigón de las vigas en T de hormigón pretensado para analizar la relación carga-deformación; la tensión del hormigón en la zona de compresión y la capacidad de carga a cortante bajo diferentes anchos de ala, las relaciones de refuerzo de los tendones pretensados y los ángulos de flexión. Los resultados experimentales se verificaron mediante los resultados de la fórmula de cálculo de la capacidad de carga especificada en China, América, Canadá y Europa. Los resultados demuestran que el aumento de la anchura del ala, el ángulo de flexión y el número de tendones pretensados puede mejorar significativamente la fuerza interna y la capacidad de carga de cizallamiento de las vigas en T. Sin embargo, la anchura del ala tiene una influencia menos evidente en la capacidad de carga de cizallamiento. El efecto positivo del ala es evidente bajo una anchura de ala específica. Por ejemplo, cuando la relación entre la anchura de la ala y la anchura del alma es superior a 4. La capacidad de carga de cizallamiento de las vigas en T de hormigón pretensado es grande cuando la relación de refuerzo y el ángulo de flexión de los tendones pretensados son grandes. Este estudio tiene valores de referencia para revelar el mecanismo de fallo por cizallamiento de las vigas en T de hormigón pretensado bajo cargas concentradas y proporciona una base para el diseño de ingeniería.
- **Palabras clave:** Hormigón pretensado, Viga T, carga de cizallamiento, Estudio experimental.

ABSTRACT

Prestressed concrete t-beams have complex shear mechanism, and their shear performance is influenced by various factors, such as flange width and prestress. The shear performance of prestressed concrete t-beams has not been solved completely. This study designed and established nine prestressed concrete t-beams and one ordinary reinforced concrete t-beam to investigate the influence of flange width and the number and bending angle of prestressed tendons on the shear bearing capacity of concrete t-beams. The crack development, failure form, mid-span deflection, and concrete strain of the prestressed concrete t-beams were measured to analyze the load–deflection relationship; the concrete strain in the compressive zone; and the shear bearing capacity under different flange widths, reinforcement ratios of prestressed tendons, and bending angles. Experimental results were verified by the outputs of the bearing capacity calculation formula specified in China, America, Canada, and Europe. The results demonstrate that the increase in flange width, bending angle, and number of prestressed tendons can improve the internal force and shear bearing capacity of t-beams significantly. However, the flange width has less evident influence on the shear bearing capacity. The positive effect of the flange is evident under a specific flange width. For example, when the ratio of the flange width to the web width is greater than 4. The shear bearing capacity of the prestressed concrete t-beams is large when the reinforcement ratio and bending angle of the prestressed tendons are great. This study has reference values for revealing the shear failure mechanism of prestressed concrete t-beams under concentrated loads and provides a basis for engineering design.

Keywords: Prestressed concrete; T-beam;Shear bearing; Experimental study.

1. INTRODUCTION

Concrete members bear axial force, bending moment, and shear force. Various complex factors influence the shear failure mechanism of oblique sections. Scholars worldwide generally proposed semi-empirical and semi-theoretical shear capacity calculation models based on the test results. The seemingly conservative design approach may exhibit security risks.

Chinese and American scholars have studied the calculation theory of shear bearing capacity of reinforced concrete beams thoroughly [1-3] and proposed many theoretical models. The calculation methods and theories have gradually advanced.

However, few studies on the shear bearing capacity of prestressed concrete beams are available. The large number of test variables complicates the manufacturing of test specimen, and the shear problem has always been a controversial and confusing problem. No model or theory can fully explain the shear mechanism. Scholars have investigated the influence of different parameters

on the shear performance of prestressed concrete t-beams [4,5]. However, the influence of flange width and prestress on the shear bearing capacity is yet to be clarified completely.

This study designed nine prestressed concrete t-beams and one reinforced concrete t-beam on the basis of the above analysis. The shear bearing capacity and shear performance of the t-beams under a concentrated load were compared and analyzed. This task is undertaken to evaluate the contribution of flange width, number of prestressed cables, and angles to the shear bearing capacity of prestressed concrete t-beams.

2. STATE OF THE ART

At present, scholars have conducted numerous studies on the shear bearing capacity of concrete beams and suggested the rationality of establishing a database for testing the shear of reinforced concrete beams and evaluating relevant code design formulas [6-8]. Deng [9] performed a test of beams without stirrups and proved the significant effects of aggregate occlusion force on the shear bearing capacity; however, the effects on the reinforced concrete and prestressed concrete beams were uninvolved. E. A. G Domínguez [10] used ANSYS to simulate load–deflection curve, ultimate load, and crack mode of the variable cross-sectional beams with stirrups in the shear test; however, the author did not analyze the prestressed concrete beams. Che et al. [11] verified the safety of the formula for the beams without stirrups based on the shear test results of large-sized beams and collected tests. They also analyzed the influence of the minimum stirrup ratio and the longitudinally distributed rebar on the shear bearing capacity of the members. However, they failed to explore the reinforced and prestressed concrete beams. Zhong [12] performed a shear failure test on five high-strength reinforced concrete beams and discussed the effects of concrete strength and stirrup ratio on the ultimate bearing capacity. Nevertheless, he did not investigate the prestressed concrete beam.

Lai [13] carried out a shear failure test on a 16-m hollow slab beam of prestressed reinforced concrete that had been used for 20 years. He also established a model by using the finite element software ABAQUS to analyze the shear performance of the hollow slab beam and the main factors that influence shear performance. His study focused on hollow slab beams rather than pre-stressed concrete T-beams. Zhang [14] carried out static loading tests on five high-performance prestressed concrete model beams and analyzed the effects of fly-ash content and concrete strength grade on the shear bearing performance of test beams. Nonlinear finite element software was also used to analyze the effects of different parameters on the shear bearing capacity. However, the influence of prestress and flange width was not analyzed. Li [15] and Li [16] tested the shear bearing capacity of prestressed concrete rectangular beams to investigate the shear failure mechanism and the main influencing factors; however, they did not explore T-beams. Considering that the prestress and compression flange can improve the shear bearing capacity, You [17] derived the formula for calculating the shear bearing capacity of prestressed concrete beams with stirrups from the truss-arch model and collected the test data for verification. However, they only focused on the prestress concrete box girder. Qi [18] discussed the shear transfer mechanism of reinforced concrete T-beams and established a theoretical calculation formula of the shear bearing capacity of concrete T-beams considering the influence of flanges; however, the influencing factors of prestress was not involved. Hong-Gun Park [19] proposed a method for analyzing the shear strength of prestressed concrete beams based on a strain–shear model. The method considered the effect of precompressive stress but neglected the beneficial effect of flange width. Eisuke Nakamura [20] used the Prestressed Concrete Shear Database of the University of Texas to verify whether the Modified Compression Field Theory (MCFT)-based shear strength expression could predict the shear bearing capacity of prestressed concrete beams accurately. Qi [21] tested nine external prestressed concrete T-beams and investigated the effects of prestress, shear–span ratio, shear reinforcement, and bending angle of the external prestressing tendons on the shear performance and shear capacity of prestressed concrete T-beams. However, the influence of the flange width of T-beams on the shear capacity was neglected.

In the present study, the experimental and finite element simulation methods were used to design and carry out the shear performance test of prestressed concrete t-beams under a concentrated load. The influence of compressed flanges and effective prestress on the shear bearing capacity was discussed from the perspectives of failure form and characteristics. The relationship between the shear bearing capacity and the effective flange width and prestress was determined. The results provide a test basis for exploring the shear mechanism of prestressed concrete beams.

The remainder of this study is organized as follows. Section III describes the design, phenomena, and results of the experiment. Section IV analyzes the test results to obtain the shear characteristics of prestressed concrete T-beams under different flange widths, bending angles of prestressed tendons, and reinforcement ratios. Finally, Section V draws the conclusions.

3.METHODOLOGY

3.1. TEST DESIGN

A T beam test was designed, and nine prestressed concrete beams and one ordinary reinforced concrete T-beam were manufactured, the specimens meet China's Concrete Structure Design Code (GB50010-2010) [22]. With the prestressed bending angle, the number of prestressed tendons, and the flange width as the parameters, the shear bearing capacity and shear performance of the prestressed concrete T-beams were studied under a concentrated load. Table I illustrates the detailed information

number	*n*(strand)	*b* (mm)	α (°)	P_{max} (kN)	number	*n*(strand)	*b* (mm)	α (°)	P_{max} (kN)
T-1	–	800	–	670	T-6	3	800	12	955
T-2	2	800	0	840	T-7	3	1080	12	967
T-3	3	800	0	950	T-8	2	800	20	881
T-4	3	1080	0	965	T-9	3	800	20	1025
T-5	2	800	12	845	T-10	3	1080	20	1040

Note: n is number of prestress tendons; b is flange width; α is bending angle; P_{max} is ultimate load.
Table. I Main design parameters of the test specimen

and main parameters of the test specimen. Figure 1 describes the reinforcement of the test specimen, the number of pore channels, and the size of the component.

The components were concreted in two concentrated time periods, namely, morning and afternoon. Moreover, 12 groups of 150 × 150 × 150mm^3 cube test blocks were cast to test the concrete strength. The cube test blocks and components were cured under the same conditions. Before the shear failure test of the prestressed tension and components, the compressive strength test was performed in the laboratory in accordance with the GB/T50081-2002 Standard for Test Methods for Mechanical Properties of General Concrete [23]. The average compressive strength f_{cu} was obtained, and the axial compressive strength f_c and tensile strength f_t were converted by calculation.

The material properties of the steel bars were measured by uniaxial tensile tests in accordance to GB/T228-2002 Tensile Test Method for Metal Materials at Room Temperature [24]. The mechanical properties of the steel bars were tested using a 100-T hydraulic tensile tester. The average yield and tensile strength of the measured steel bars were used to determine the yield and tensile strength of each type of steel bar. The prestressed steel strands are 7Φ5 steel strands manufactured by Xiangtan Steel Strand Company. The standard values of tensile strength are f_{ptk} = 1860 N/mm^2 and E_s = 1.95x10^5 MPa.

3.2 TEST LOADING AND MEASUREMENT

The main test contents of the T test include the appearance and the strain.The test points are arranged according to the aforementioned test contents.

1) A 3 mm × 5 mm steel bar gauge was affixed to the mid-span position of longitudinal reinforcement to study the variation law of longitudinal reinforcement stress.
2) The average strain of the stirrups between the loading point and the support was measured to study the variation law of their stress in the shear span region. A 3 mm × 5 mm steel bar gauge was arranged in the middle of each stirrup.
3) A pressure sensor was installed at the anchor end to obtain the tension control force under the anchor to grasp the prestress magnitude and prestress loss accurately.
4) A 3 mm × 80 mm concrete strain gauge was arranged along the line that connects the load point and the support in the shear compression and span zones.
5) A dial indicator was installed at the support and quartile at both ends of the T-beam to measure the load–deflection curve of the prefabricated T-beam. One dial indicator was installed in the beam span to record the displacement of the beam at the mid-span, quartile, and support under each load.

A rigid reaction force frame was used to erect the jack for vertical top-bottom loading, and movable and fixed hinge supports assisted the components on two rigid piers in Figure 2. Multistage loading was performed, and the load was exerted from the cracking load to the cracking load with a level of 20 kN until the concrete cracked with a level of 10 kN. The T-beam was loaded with a level of 20 kN. At 80% of the calculated failure load, the T-beam was loaded with a level of 10 kN until the failure load occurred. The load was held for 3 min.

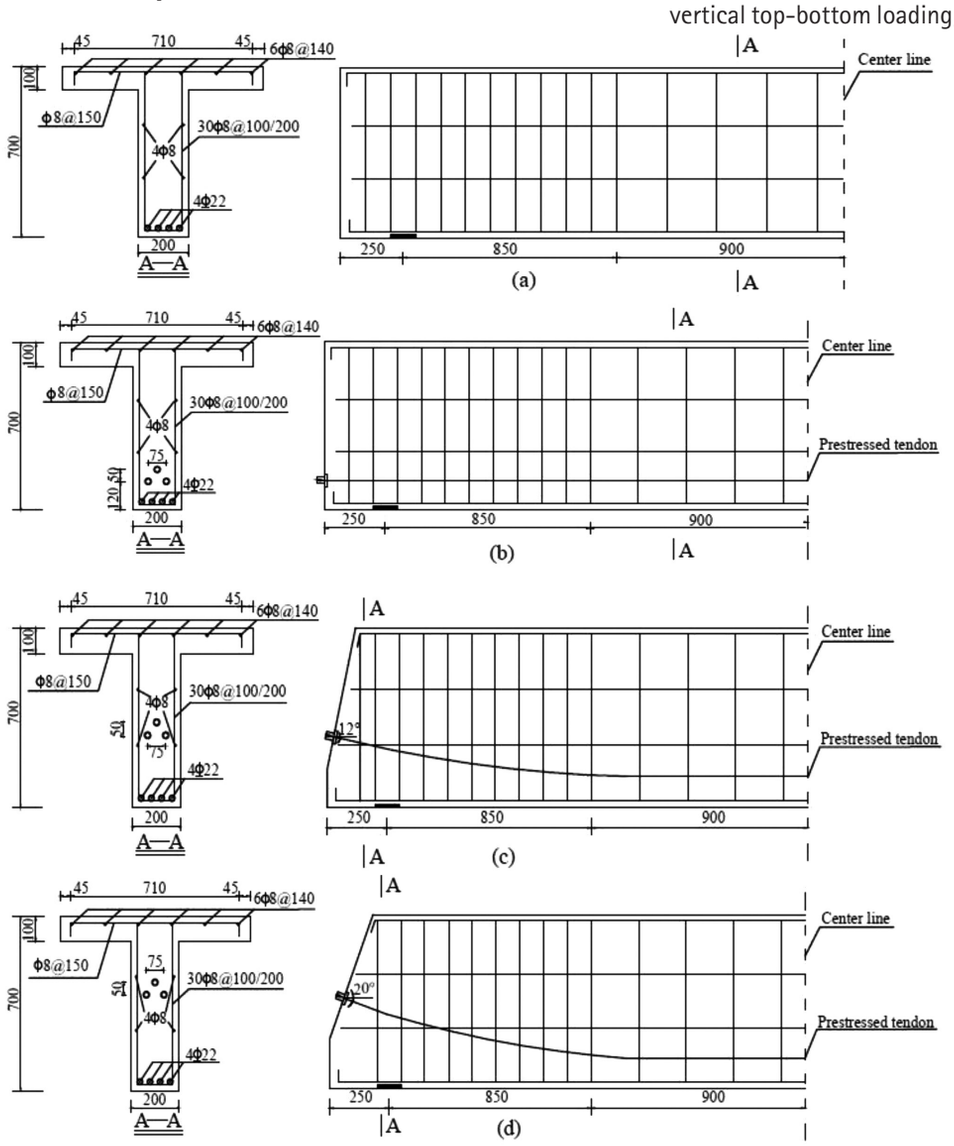

Fig.1. Size and reinforcement of components.(a) Reinforced concrete T-beam. (b) Prestressed T-beam with an angle of 0°. (c) Prestressed T-beam with an angle of 12°. (d) Prestressed T-beam with an angle of 20°

3.3 TEST PHENOMENA AND RESULTS

The first vertical crack of the T-1 beam appeared when the mid-span load P was 160 kN. The diagonal crack appeared at the load of 200 kN which further extended and developed from the mid-span to the two supports in a splayed shape. The critical diagonal cracks were formed as the load increased further. When loading to 670 kN, the load indicator showed a downward trend of the load, but the cracks continued to develop. Therefore, the beam had been damaged.

In the T-2–10 beams, the initial oblique crack was close to the mid-span position and slowly developed toward the

support, all of which pointed toward the loading point. With the further increase in load, the critical oblique cracks were formed, and the crack width and number gradually increased. With the further increase in load, the critical diagonal cracks became wide rapidly, some cracks developed from the critical oblique cracks to the horizontal direction, and the cracks on the flange almost penetrated the sectional height. When the ultimate load was reached, the load sharply dropped, and the concrete in the compression zone was crushed, thereby resulting in shear failure of the specimen.

Shear failure occurred in all specimens, and the cracks were mainly oblique ones. The cracks were mainly concentrated at the web of the T-beam. Fig. 3 shows the distribution and failure state of cracks in all specimens, the thick black line represents the critical inclined crack.

The failure mode manifests that the inclination angle of the critical oblique crack of specimen T-1 was basically 45°. Meanwhile, the inclination angles of the oblique cracks of prestressed concrete specimens T-2–T-10 were significantly smaller than 45°, and the cracking time of T-beams equipped with prestressed tendons was delayed, the compressive stress distribution in the flange plate was uneven. The inclination angle of the critical oblique crack of the specimen with great prestress and large bending angle was gentle. The inclination angles near the bottom of the beam were small, and some angles were even horizontal. The cracks around the critical oblique crack were dense.

Fig. 2: Test loading device

4. RESULT ANALYSIS AND DISCUSSION

4.1 LOAD-DEFLECTION CURVE

Figure 4 presents the load-deflection curve of the test specimen, figure 4 (a) presents the load-deflection curve of t-beams with 2, 2, 3 strand prestressed bars and flange width 800 mm, 800 mm, 1080 mm at bending angle of prestressed tendons 0°, 12° and 20° respectively.

1) Before cracking, the load–deflection curve changed linearly, and the cracking of T-beams with prestressing tendons was later than that of the T-1 beam. After the cracks entered the nonlinear stage, and the failure load was approached, the deflection increased sharply, the bearing capacity was lost, and failure occurred.
2) The ultimate shear capacities of the T-2, T-5, and T-8 specimens equipped with prestressing tendons were increased by 25.37%, 26.12%, and 31.49%, respectively, compared with T-1. As the bending angle increased from the horizontal level to 12°, the ultimate shear bearing capacity of T-5 was not much higher than that of T-2. However, when the bending angle increased to 20°, the shear bearing capacities of T-8 were 4.88% and 4.26% higher than those of T-2 and T-5, respectively.
3) Increasing the number of prestressing tendons can significantly improve the ultimate shear bearing capacity of the t-beam. The shear bearing capacity of T-3, T-6, and T-9 with three prestressing tendons was increased by 13.1%, 13.02%, and 16.35% compared with T-2, T-5, and T-8, respectively.

4.2 ANALYSIS OF CONCRETE STRAIN IN COMPRESSIVE ZONE

Figure 5 shows the changes in the position and strain of the concrete strain measurement point in the compression zone at the top of the prestressed concrete T-beams, H is measurement points of concrete strain in compression zone, solid lines depict the actual measurement, dotted line depict the simulated result. Before the diagonal cracks appeared in the specimen, the strain on the concrete at the top of the beam linearly increased with the load. After the cracks appeared, the concrete in the tension zone gradually withdrew, and the neutral axis at the crack cross-section moved up. The concrete in the compression zone underwent plastic deformation, and the strain gradually increased, showing a nonlinear change trend. The neutral axis further moved up, and the cracks extended upward and expanded with the continued increase in load. The plastic characteristics became increasingly obvious. When the compressive stress reached the compressive strength of the concrete, the concrete strain in the compression zone peaked, and the strain gradually decreased until the concrete in the compression zone was crushed.

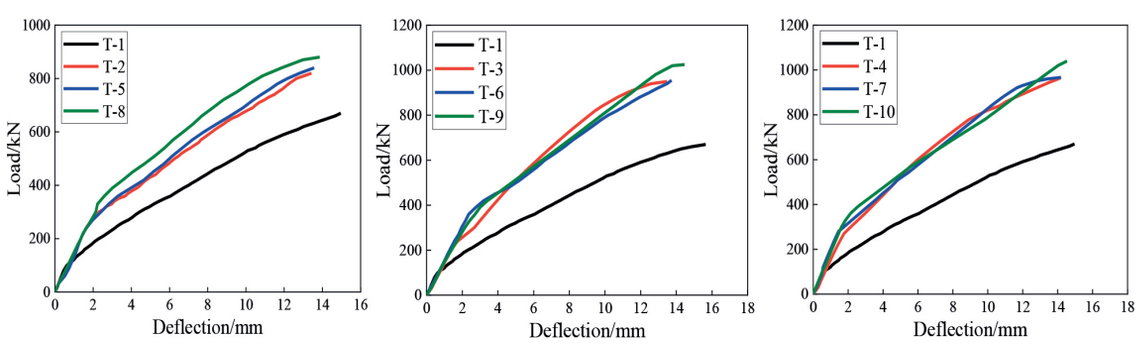

Fig. 4: Load-deflection curve. (a) two strand prestressed bars and flange width 800 mm. (b) three strand prestressed bars and flange width 800 mm.(c) three strand prestressed bars and flange width 1080 mm

Since the compressive stress of web will be transferred to the flange, and the shear stress is not evenly distributed on the flange plate, the shear stress is the largest at the junction of the web and flange, and the stress gradually decreases staying away from the web, which resulting in the shear lag effect. Therefore, there was a critical horizontal oblique crack along the interface between the web and flange when the specimen is damaged by shear pressure, and the reason is why the crack at the lower edge of the flange does not extend to the edge of the flange when the flange is damaged by compression.

In order to validate analytical results, finite element software ABAQUS was used to model steel and concrete separately,both are coupled by embedded method, non-linear parameters of the materials were taken into account, model results were included in figure 5.

4.3 EFFECT OF THE FLANGE ON THE SHEAR CAPACITY

The test results demonstrates that when the flange expanded, the shear bearing capacity slightly increased. When the bending angles were α_p=0°, α_p=12°, and α_p=20°, they were increased by 1.58%, 1.26%, and 1.46%, respectively. The numerical change is completely within the randomness of the test and the range of the test error, which cannot reflect the influence of the flange width on the shear bearing capacity.

The influence of flange width on the shear bearing capacity of prestressed concrete T-beams was studied to make up for the lack of data in the test. Finite element software ABAQUS was used to simulate the shear of the members with flange widths of 200, 400, and 600 mm under the concentrated force. The whole beam body was meshed by 50 mm × 50 mm, steel and concrete were connected by means of embedded technology, the tension of prestressed steel bar was simulated by applying temperature drop to the cable element to generate shrinkage strain. Table II presents the simulated and experimental values of the shear bearing capacity under different flange widths.

According to the datas the increase in the shear bearing capacity was evident when the bending angle of the prestressed tendons was great. When the bending angle was α_p=20°, the shear bearing capacity was 13.2%, the ratio of the flange width to the web width b/b_w increased from one to four, and the shear capacity was greatly improved. When α_p=0°, 12°, and 20°, the increase rates were 10.1%, 8.8%, and 11.5%, respectively. However, the shear bearing capacity exhibited almost no change when b/b_w increased from 4 to 5.4. Increasing the flange width had minimal influence on the shear bearing capacity. When b/b_w = 4, the flange width greatly contributed to the shear bearing capacity. The flange width has a limited effect on the shear bearing capacity. The critical value for the beneficial effect of flange width on shear bearing capacity is b/b_w = 4.

The test datas of 90 groups of the prestressed t-beams and 120 groups prestressed concrete rectangular beams was screened from shear database[6] [8], the results show that the shear strength increased with the increase of b/bw, after the b/b_w> 5, the growth trend of shear strength is slowing down. Thus it can be seen that the effect of flange on the improvement of shear bearing capacity is limited, flange influence on shear bearing capacity is no longer so obvious after a certain width, this is basically consistent with the experimental results in this paper.

Bending angle	Simulation results (kN)			Test results (kN)	
	200mm	400mm	600mm	800mm	1080mm
0°	863	882	906	950	955
12°	868	889	910	955	967
20°	919	937	973	1025	1040

Table II: Simulation results and test results

4.4. EFFECTS OF PRESTRESSED REINFORCEMENT RATIO ON THE SHEAR BEARING CAPACITY

Figure 6 shows the load–displacement curves under different prestressed reinforcement ratios, figure 6 (a), (b), (c) presents the load-deflection curve of t-beams with bending angle of prestressed tendon 0°, 12° and 20° and flange width 800 mm at two and three prestressed bars respectively, where ρ_{pb} is ratio of prestressed reinforcement. When the bending angles of the prestressed reinforcement were α_p=0°, 12° and 20°, the shear bearing capacities of the three prestressed tendons were increased by 13.1%, 13.69%, and 16.35%, respectively, compared with the two prestressed tendons. The turning point of the curve was high when the prestressed reinforcement ratio was large. This situation indicates that prestress can change the internal stress of the components from the internal mechanism. The prestress can not only delay the cracking time and inhibit the crack development but also increase the area of the shear compression zone and change the direction of the main tensile stress. The oblique cracks are sufficiently gentle to run through stirrups and enhance the cracking load and the ultimate shear capacity of the T-beam.

4.5 EFFECTS OF EFFECTIVE PRESTRESS ON THE SHERA BEARING CAPACITY

Figure 7 demonstrates that the effective prestressing can significantly improve the shear bearing capacity of the component, figure 7(a), (b), (c) presents the load-deflection curve of t-beams with bending angle of prestressed tendons 0°, 12° and 20° at different flange width and prestress force respectively, where $\rho_{ñ}$ is effective prestress force. When the prestressing bars were arranged horizontally, the shear bearing capacity of T-4 was 14.9% higher than that of T-2. In the case of α_p=12°, the shear bearing capacity of T-7 was 14.4% higher than that of T-5. When α_p=20°, the shear bearing capacity of T-10 was 18% higher than that of T-8. Effective prestress has significant effects on the shear bearing capacity. Large effective prestress can increase the axial force, improve the aggregate occlusion mechanism of the cracked section, and increase the height of the shear zone of the component. Moreover, such stress can reduce the crack cracking time, decrease the crack width, and effectively improve the shear bearing capacity of the component.

The specification[22] [25]stipulates the upper limit value of the contribution of prestress to the bearing capacity, when N_p>0.3 f_c A_0, the beneficial effects of prestress are on the decline. In this article the maximum effective prestress value $N_{ñmax}$=474 kN <0.3 f_c A_0=829kN, the contribution of prestress is obvious, which is in accordance with the regulations.

4.6 CALCULATION OF THE BEARING CAPACITY

Before the specimens were examined according to the calculation formula of the shear bearing capacity, concrete strength should be first converted. The Chinese and European codes use the strength of the cube specimen as the basic index of concrete strength. Meanwhile, the United States and Canada codes take the characteristic value of the compressive strength of the cylindrical test piece to determine the strength level of the concrete. In literature [26], the following formula is used:

$$f_c^{'} = 0.8 f_{cu} . \quad (1)$$

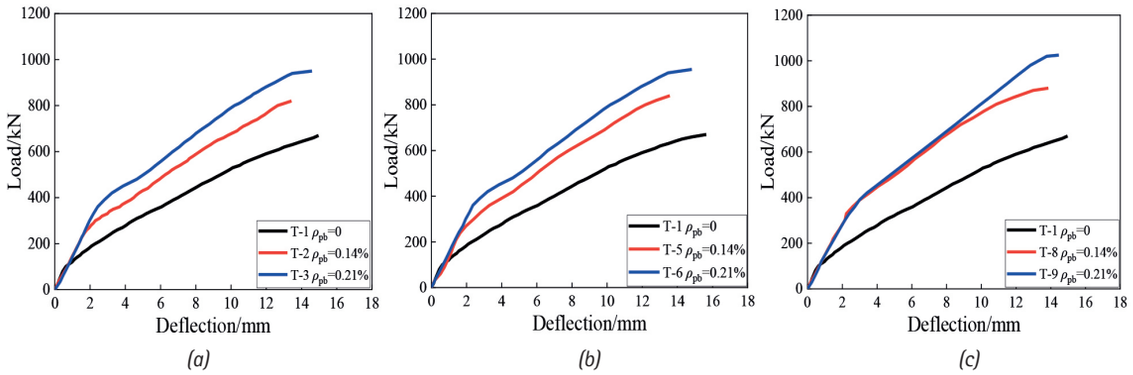

Fig. 6: Load-deflection curve. (a) 0°. (b) 12°. (c) 20°

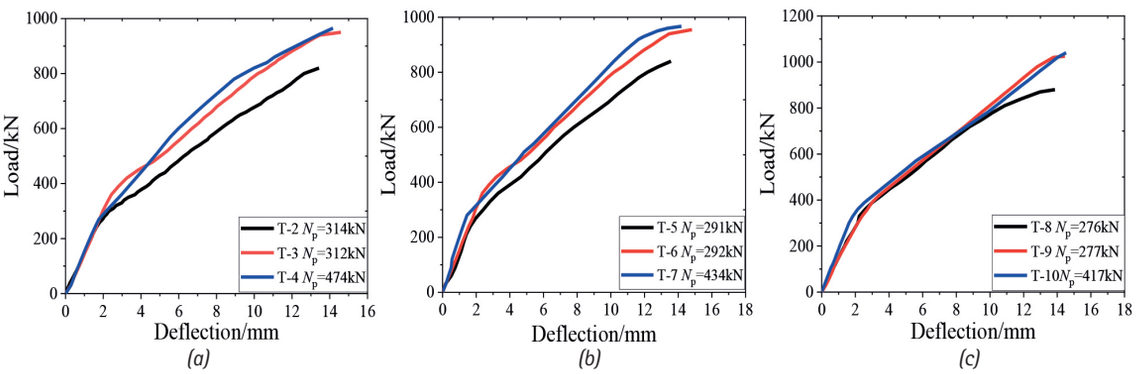

Fig. 7: Load-deflection curve. (a) 0°. (b) 12°. (c) 20°

Number	V_{test} (kN)	Calculated value of specimens in each country V_{test} / V_{cal}					
		GB50010-2010	JTG3362-2018	ACI318-19	AASHTO-2017	EN 1992-1-1:2014	CSA A 23.3-04
T-1	670	1.32	1.35	1.28	1.42	1.47	1.36
T-2	840	1.34	1.34	1.33	1.38	1.58	1.42
T-3	950	1.33	1.37	1.30	1.41	1.59	1.49
T-4	965	1.34	1.38	1.28	1.42	1.61	1.49
T-5	845	1.29	1.18	1.29	1.29	1.55	1.21
T-6	955	1.24	1.2	1.25	1.21	1.4	1.23
T-7	967	1.25	1.21	1.24	1.2	1.41	1.22
T-8	881	1.21	1.15	1.31	1.28	1.51	1.17
T-9	1025	1.2	1.22	1.29	1.33	1.46	1.2
T-10	1040	1.22	1.19	1.29	1.31	1.46	1.19
Average value		1.27	1.26	1.29	1.33	1.5	1.3
Coefficient of variation		0.13	0.21	0.1	0.19	0.15	0.29

Table III. Comparison of test values and calculated values

where $f_c^{'}$ is compressive strength of concrete, f_{cu} is compressive strength of concrete cube .

Table III compares the test values and calculation results according to the codes. The calculation results of the standard formula have sufficient safety reserves, but those of the specifications of different countries vary. The values calculated according to China's Concrete Structure Design Code (GB50010-2010) [22], Highway Reinforced Concrete and Prestressed Concrete Bridge and Culvert Design Code (JTG3362-2018) [27], and the American Concrete Structure Design Code (ACI318-19) [25] are similar. The influencing coefficient of the flange width and the increase coefficient of prestress are explicitly considered in the Chinese Bridge Design Code. Accordingly, the calculated value of the bridge code is closer to the test value. The calculation results of the American Code for Design of Highway Bridges (AASHTO-2017) [28] and Canadian Concrete Code (CSA A 23.3-04] [29] are safe. Meanwhile, the calculation results of the European Code for Design of Concrete Structures (EN1992-1-1:2014) [30] are conservative. The calculated coefficient of variation of United States ACI318-19 is 0.1 according to the coefficient of variation. Such value is stable and can predict the test results accurately.

5. CONCLUSION

The present study aims to explore the shear mechanism of prestressed concrete t-beams under the action of concentrated force and reveal the relationship between the shear bearing capacity of prestressed concrete t-beams and the flange width and prestress. This study used experimental and numerical simulation methods to analyze the shear bearing capacity and shear performance of prestressed concrete t-beams when the changes in flange width, bending angle, and reinforcement ratio of prestressed tendons occur. The following conclusions could be drawn:

1) Prestress significantly improves the mechanical performance and the crack resistance of the components and delays the appearance of cracks in the concrete t-beam. In addition, prestress significantly reduces the width of the cracks, increases the stiffness of the concrete t-beam, and improves the shear bearing capacity of prestressed concrete t-beam.
2) The prestressing angle and reinforcement ratio of the prestressed tendons can not only significantly improve the

internal force of the prestressed concrete T-beam but also greatly increase the shear bearing capacity of the prestressed concrete T-beams. Although increasing the flange width can augment the concrete area in the compressive zone, the influence of flange width on the shear bearing capacity is limited. When b/b_w = 4, the shear bearing capacity is unaffected by the flange width.

3) The comparison outcome shows that the test results are larger than the calculation results. The calculation results of the code formula have sufficient safety reserves. However, the results calculated according to the codes of different countries are vary. The Chinese Bridge Design Code can predict the test results accurately, while the calculated value of the American ACI specification is stable.
4) The shear mechanism of prestressed concrete t-beams can also be explained by strut-and-tie model, which will be obtained in subsequent studies.

This study proposed a new understanding of the shear mechanism of prestressed concrete T-beams based on the combination of experiments and theoretical research. The designed tests are close to the actual engineering and have certain reference significance for studying the shear mechanism of prestressed concrete beams. Effective prestress should be measured in subsequent studies accurately because of the lack of advanced equipment and effective measurement methods.

REFERENCES

[1] Wu W K, Hsu T T C, Hwang S J. "Shear strength of reinforced concrete beams". ACI Structural Journal, July 2014. Vol. 111-4, p.809-818. DOI: http://dx.doi.org/10.14359/51686733.
[2] Yi Weijian. Experimental and theoretical research on concrete structures. Beijing: Science Press, 2012. p.256-258. ISBN: 9787030354471.
[3] Lee J Y, Lee D H, Lee J E, et al. "Shear behavior and diagonal crack width for reinforced concrete beams with High-strength shear reinforcement". ACI Structural Journal, May 2015. Vol. 112-3, p.323-333. DOI: http://dx.doi.org/10.14359/51687422.
[4] Arghadeep Laskar, Thomas T. C. Hsu, and Y. L. Mo. "Shear Strengths of Prestressed Concrete Beams Part 1:Experiments and Shear Design Equations". ACI Structural Journal, May 2010. Vol. 107-3, p.330-339. DOI: http://dx.doi.org/10.14359/51663698.
[5] Ioannis P. Zararis, Maria K. Karaveziroglou, and Prodromos D. Zararis. "Shear Strength of Reinforced Concrete T-Beams". ACI Structural Journal, September 2006. Vol. 103-5, p.693-700. DOI: http://dx.doi.org/10.14359/16921.
[6] Karl-Heinz Reineck, Evan Bentz, Birol Fitik, Daniel A. Kuchma, and Oguzhan Bayrak. "ACI-DafStb database for shear tests on slender reinforced concrete beams with stirrups". ACI Structural Journal, September 2014. Vol. 111-5, p.1147-1156. DOI: http://dx.doi.org/10.14359/51686819.
[7] Reineck K H, Todisco L. "Database of shear tests on non-slender reinforced concrete beams without stirrups". ACI Structural Journal, November 2014. Vol. 111-6, p.1363-1372. DOI: http://dx.doi.org/10.14359/51686820.
[8] Todisco L, Reineck K H, Bayrak O. "Database with shear tests on non-slender reinforced concrete beams with vertical stirrups". ACI Structural Journal, November 2015. Vol. 112-6, p.761-769. DOI: http://dx.doi.org/10.14359/51688055.
[9] Q Deng, W J Yi, F J Tang. "Effect of Coarse Aggregate Size on Shear Behavior of Beams without Shear Reinforcement". ACI Structural Journal, September 2017. Vol. 114-5, p.1131-1142. DOI: http://dx.doi.org/10.14359/51689720.
[10] Godínez-Domínguez E A, Tena-Colunga A, Juárez-Luna G. "Nonlinear finite element modeling of reinforced concrete haunched beams designed to develop a shear failure". Engineering Structures, December 2015. Vol. 105-1, p.99-122. DOI: http://dx.doi.org/10.1016/j.engstruct.2015.09.023.
[11] Che Yi, Yu Lei. "Research on safety of large-scale reinforced concrete members without web tendons under shear force" . Journal of Building Structures, February 2014. Vol. 35-2, p.144-151.
[12] Zhong Jibo. Study on the shear performance of high-strength reinforced high-strength concrete beams based on concentrated load. Nanning: Jiangsu University, June 2018.
[13] Lai Jinlong. Shearing performance analysis of existing prestressed concrete hollow slab beams. Harbin: Northeast Forestry University, 2018.
[14] Zhang Zhipei. Study on Shear Performance of Prestressed High Performance Concrete T Beams. Shijiazhuang: Shijiazhuang Railway University, June 2016.
[15] Li Hao. Shear capacity of prestressed concrete beams and improved truss arch model. Dalian: Dalian University of Technology, June 2014.
[16] Li Guanquan. Numerical simulation and analysis of shear failure of prestressed concrete beams. Guangzhou: South China University of Technology, May 2014.
[17] You Fangchen. Study on Shear Properties of Prestressed Concrete Beams. Nanjing: Southeast University, April 2015.
[18] Qi Jianan, "Wang Jingquan. Shear capacity of reinforced concrete t-beams considering flange effects" [J]. Journal of Southeast University, July 2019. Vol. 49-4, p.638-644.
[19] Hong-Gun Park, Soonpil Kang, Kyoung-Kyu Choi. "Analytical model for shear strength of ordinary and prestressed concrete beams". Engineering Structures, January 2013. Vol. 46, p.94-103. DOI: http://dx.doi.org/10.1016/j.engstruct.2012.07.015.
[20] Eisuke Nakamura, Alejandro R. Avendano, and Oguzhan Bayrak. "Shear Database for Prestressed Concrete Members". ACI Structural Journal, November 2015. Vol. 110-6, p.909-918. DOI: http://dx.doi.org/10.14359/51686147.
[21] Jia-Nan Qi, Jing-Quan Wang, Zhongguo John Ma, et al. "Shear Behavior of Externally Prestressed Concrete Beams with Draped Tendons". ACI Structural Journal, July 2016. Vol. 113-4, p.677-688. DOI: http://dx.doi.org/10.14359/51688746.
[22] Code for design of concrete structures: GB50010-2010. Beijing: China Construction Industry Press, 2010.
[23] Standard for test methods of mechanical properties of ordinary concrete: GB/T 50081—2002. Beijing: China Construction Industry Press, 2003.
[24] Tensile test method for metal materials at room temperature: GB/T 228-2002. Beijing: China Standard Press, 2003.
[25] ACI Committee 318, Building Code Requirements for StrucTural Concrete (ACI 318-19) and Commentary. American Concrete Institute, Farmington Hills, MI, August 2019. DOI: http://dx.doi.org/10.14359/51716937.
[26] Guo Zhenhai, Shi Xudong. Principles and Analysis of Reinforced Concrete. Beijing: Tsinghua University Press, 2003. p.14. ISBN: 9787302071921.
[27] Design code for highway reinforced concrete and prestressed concrete bridges and culverts: JTG 3362-2018. Beijing: People's Communications Press, 2018.
[28] AASHTO LRFD Bridge Design Specifications. American Association of State and Highway Transportation Officials, WashingTon, DC, 2017.
[29] CSA Committee A23.3, Design of Concrete Structures (CSA A23.3-04) and Commentary. Canadian Standards Association Mississauga, Ontario, 2004.
[30] EN 1992-1-1:2004, Eurocode 2: Design of Concrete Structures. General Rules and Rules for Buildings. London: British Standards Institutions, December 2014. DOI: http://dx.doi.org/10.3403/03178016.

APPRECIATION

This work was supported by National Natural Science Foundation of China (51338004), Outstanding Youth Project of Hunan Provincial Education Department (18B437), and Innovation and Entrepreneurship Training Program for College students of Hunan Province (S201911527034)

SUPPLEMENTARY MATERIAL

https://www.revistadyna.com/documentos/pdfs/_adic/9655-1.pdf